

A. Manonmani¹ / T. Thyagarajan² / S. Sutha²

Evolutionary Algorithm-Based Multi-objective Control Scheme for Food Drying Process

¹ Department of Electronics and Instrumentation Engineering, Saveetha Engineering College, Chennai, E-mail: manoraj1983@gmail.com

² Department of Instrumentation Engineering, MIT Campus, Anna University, Chennai

Abstract:

Food drying is one of the important methods to prevent microbial growth during preservation. However, it is a complex non-linear process where the quality of the food depends on environmental conditions. Therefore, food drying must be carried out under controlled environment. In this paper, an internal model control (IMC) scheme is developed for pineapple drying using the evolutionary algorithms namely: genetic algorithm (GA) and particle swarm optimization (PSO) to achieve the desired quality (single objective). In order to reduce the control effort and hence the cost, without compromising the desired quality, a multi-objective control scheme is also formulated using weighted sum method. The closed loop performance of the control scheme for GA-based IMC-PI controller and PSO-based IMC-PI controller are analyzed for servo and regulatory operations. The results thus obtained are compared both qualitatively and quantitatively. From the simulation results it is observed that PSO-based IMC-PI controller gives better performance and better range of the temperature compared to the other control schemes.

Keywords: food drying, multi-objective control, evolutionary algorithm and internal model control

DOI: 10.1515/ijfe-2016-0219

1 Introduction

Drying is one of the important operations in the food processing. Many physical, chemical and nutritional changes occur in food materials during the dehydration process. Food products are heat sensitive and experience shrinkage making the process more complex. Many of these changes are functions of temperature, moisture content and time. Ventilation is the process in which the supply of high-quality cool air is used in the food drying process (FDP) for the removal of moisture. Hence, it is necessary to understand the temperature and moisture aspects in order to design an effective control scheme for drying of food materials.

Mathematical models are very useful in the design and analysis of simultaneous heat and moisture transfer processes in FDP. Drying models can be divided into three major groups: (a) those involving empirical equations valid for specific processes; (b) those based on basic heat and mass diffusion models forming systems of simultaneous equations and (c) a group of more comprehensive models that associate with energy, mass and momentum transport equations with all the thermodynamic laws [1].

There are many methods available for drying food materials in FDP. They are direct drying, indirect drying, dielectric drying, freeze drying, supercritical drying and natural air drying. Bulet Yestitala and Mehmet Azmi Aktair proposed a simple moisture transfer model for drying sliced food [2]. The drying of thin sliced pineapple with the help of oven dry bulb temperature has been proposed with a blanching temperature and time constraints [3]. Lee Woun Tan et al proposed a spray drying process for an orange juice powder using a nozzle spray dryer. In the case of direct drying [4], the heating of air increases the driving force for heat transfer and accelerates drying. This type of direct drying is also called a spray drying. In Ref. [5], to develop and validate computation fluid dynamics (CFD) model to predict the temperature profile during the thermal processing of this sample in a glass jar. In Ref. [6], the mathematical model for CFD for canned pineapple slices and to reduce the size of the fruit was developed and explained. In the indirect drying, heating through a hot wall is done with the help of drum. The processing time for indirect drying is longer. The increase in the temperature will automatically speed up the drying. Dielectric drying is based upon the radiofrequency or microwave in which moisture is being absorbed inside the material.

Freeze drying [7] is a drying method where the solvent is frozen by passing the gas phase directly to the solid phase below the melting point of the solvent. This is done at low temperatures outside the drying chamber. In

A. Manonmani is the corresponding author.

©2017 by De Gruyter.

This content is free.

supercritical drying process, a steam is passed to the food products containing water by which the water content is boiled off. In the case of natural air drying, the food materials are dried with the help of unheated forced air. This process is slow and weather dependent.

In most of the papers related to drying, the controller used was conventional PI controller. In spray drying [4] of orange juice powder, the PI controllers were tuned by direct synthesis method. The batch fluidized bed dryer reported in [8], a PI controller is tuned for a minimum square error. In this paper a conventional and improved version of IMC-based PI controller schemes are proposed for drying a sliced pineapple. Then multi-objective IMC-based PI controller is fine-tuned using genetic algorithm (GA) and particle swarm optimization (PSO) to get the desired performance and minimum control effort (CE).

In the natural drying process, sliced fruits are dried by exposing them in solar radiation for more days. However, in this process the fruits sliced are suffered by some undesirable effects namely: dust, dirt, and atmospheric pollution and insects attacks. Because of the limitations, the quality of the product gets degraded. Hence, automatic control scheme is essential for drying process.

The main objectives of the control scheme developed for drying to achieve the desired drying quality with minimum cost. In the closed loop control system, the desired quality and cost depend on integral square error (ISE) and control effort (CE) respectively. However, these two are conflicting objectives. In order to achieve the desired quality one has to be compromise on cost. The drastic variation in temperature and humidity may destroy the sliced fruit. Hence, formulation of multi-objective control problem is essential for drying process.

This paper is organized as follows: Section 2 briefly describes the mathematical model of drying process for sliced pineapple. The linearization details are presented in Section 3. The design of different control schemes is explained in Section 4 followed by a discussion of the closed loop analysis in Section 5. Finally, the conclusions are presented in Section 6.

2 Mathematical modeling of drying process for sliced pineapple

The mathematical model for the FDP includes: heating model and ventilating model. The main purpose of ventilation is to regulate the temperature at the optimum level, to ensure the movement of air and to ensure a fresh supply of air. The heating model is essential, when the inside temperature of the dryer is very low during winter and at night time. The heating is done to remove the moisture content from the food materials. The block diagram for sliced pineapple drying arrangement is shown in Figure 1.

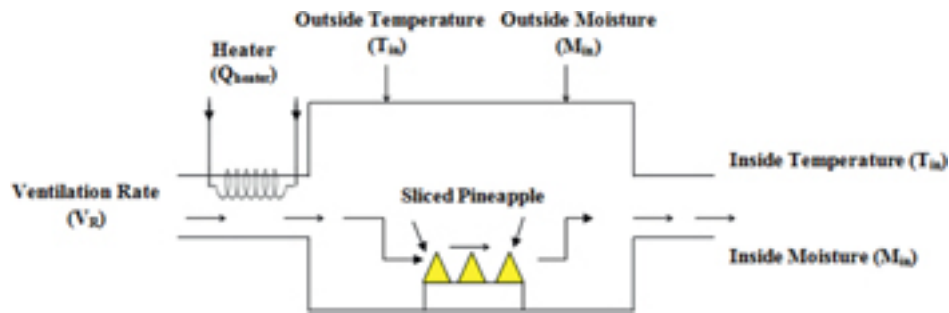


Figure 1: Block diagram for sliced pineapple drying arrangement.

From Figure 1, the inputs to the FDP are ventilation rate and heater; outputs are inside temperature and inside humidity of the air in the FDP and the disturbances are outside temperature and outside humidity

The mathematical model for drying a sliced pineapple is obtained by combining heating and ventilation model as follows:

$$\left. \begin{aligned} \frac{d}{dt} T_{in}(t) &= \frac{1}{DC_a V_T} [Q_{heater}(t)] - \left(\frac{V_R(t)}{V_T} + \frac{HT}{DC_a V_T} \right) \cdot T_{in}(t) \\ &\quad - \left(\frac{V_R(t)}{V_T} + \frac{HT}{DC_a V_T} \right) \cdot T_{out}(t) \\ \frac{d}{dt} M_{in}(t) &= -\frac{V_R(t)}{V_H} M_{in}(t) - \frac{V_R(t)}{V_H} M_{out}(t) \end{aligned} \right\} \quad (1)$$

During the drying of sliced pineapple, inside temperature for the dryer should be maintained in the range of 35 °C to 65 °C and the inside moisture in the range of 45 % to 14 %. The heater is used to supply heat during drying and the ventilation is to provide the air to circulate inside the drying chamber in order to maintain the temperature in the desired level.

The parameters and control variables are normalized as follows: $C = DC_a V_T$, $\alpha' = \alpha / (\lambda V_H)$, $\lambda' = \lambda Q_{\text{heater}}^{\max}$, $V' = V_H / Q_{\text{heater}}^{\max}$, $V_{R,\%} = V_R / V_R^{\max}$ and $Q_{\text{heater},\%} = Q_{\text{heater}} / Q_{\text{heater}}^{\max}$.

The operation conditions for drying of sliced pineapple are shown below in Table 1.

Table 1: Operating conditions used in drying of sliced pineapple.

Parameters	Value with Units
Indoor air temperature, T_{in}	35 °C to 65 °C
Outdoor air temperature, T_{out}	25 °C
Interior moisture, M_{in}	45 % to 14 %
Exterior moisture, M_{out}	4 %
Heat transfer coefficient of enclosure, HT	29.81 WK ⁻¹
$C = DC_a V_T$	324.67 minW°C-1
Active mixing volume of temperature and moisture (V_T and V_H)	60–70 %
Ventilation Rate (V_R)	0–2 (m ³ /s)
Heat provided (Q_{heater})	0–2 (W)
Air density, D	1.2 kg/m ³
Specific heat of air, C_a	1,006 J/(kg K)

By representing eq. (1) in the state-space form:

$$\begin{cases} \dot{x}_1(t) = \frac{UA}{D} u_2(t) - \frac{1}{V_T} u_1(t) + \frac{UA}{D} x_1(t) - \frac{UA}{D} v_2(t) \\ \dot{x}_2(t) = -\frac{1}{V_H} x_2(t) + \frac{1}{V_H} u_1(t) v_2(t) + \frac{1}{V_H} u_1(t) x_2(t) \end{cases} \quad (2)$$

where $x_1(t)$ is inside temperature, $x_2(t)$ is inside moisture, $u_1(t)$ is ventilation rate, $u_2(t)$ is heater input, $v_1(t)$ is outside temperature, $v_2(t)$ is outside moisture.

2.1 Relative gain array analysis (RGA)

From the state-space form represented in eq. (2), the pairing of input and output is derived and accordingly the values of the system (A), input (B) and output (C) matrices are obtained as follows:

$$A = \begin{bmatrix} -\frac{UA}{D} & 0 \\ \left(-\frac{V_R}{V_T}\right) x_2 + \frac{HT}{DC_a V_T} v_2 & -\frac{1}{t_v} \end{bmatrix}$$

$$B = \begin{bmatrix} \left(-\frac{1}{V_T}\right) x_1 + \frac{1}{t_v} v_2 & -\frac{\lambda'}{D} \\ \left(-\frac{1}{V_T}\right) x_2 + \frac{1}{t_v} v_2 & \frac{1}{V'} \end{bmatrix}$$

$$C = \begin{bmatrix} 1 & 0 \\ 0 & 1 \end{bmatrix}$$

$$\Lambda = \begin{bmatrix} 0.8162 & 0.1832 \\ 0.1832 & 0.8162 \end{bmatrix}$$

From the RGA analysis it is observed that the relative gains are positive values. If $0 < \lambda_{11} < 1$, then there is an interaction. From the interaction analysis, it is found that y_1 is paired with u_1 , and y_2 is paired with u_2 to form two loops. The disturbance occurring in one loop will affect the response of the other loop due to coupling. Hence, decoupling is necessary for this process. The feedback-feedforward linearization technique used for disturbance decoupling is discussed in the subsequent section.

3 Feedback-feedforward linearization technique

The feedback-feedforward linearization technique used for linearization and decoupling for systems with external disturbances technique is proposed by Isidori [9].

The block diagram of the closed loop control strategy for the pineapple slice drying is shown in Figure 2.

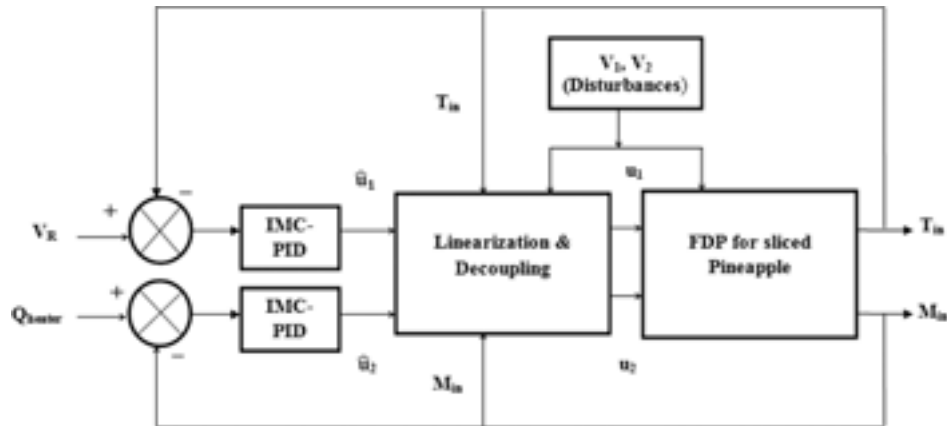


Figure 2: Closed loop control strategy for sliced pineapple drying.

The FDP is a multivariable system. The inputs to the FDP are the ventilation rate (V_R) and heater input (Q_{heater}). The external disturbances include: outside temperature (V_1) and outside moisture (V_2). The outputs from the FDP are: inside temperature (T_{in}) and inside moisture (M_{in}). \hat{u}_1 and \hat{u}_2 are the temperature change and moisture change. u_1 and u_2 are the control variables. Generally the closed loop responses of the multivariable FDP are affected by the disturbance variables namely: outside temperature and outside moisture. The decoupled and linearized model that is developed from the desired closed loop using feedback-feedforward linearization based on the model IMC controller is designed. From the state-space representation for food drying process expressed in eqs (2), the feedback-feedforward linearization and decoupling procedure is followed and the compensator is designed. The compensator for the process input control variables u (u_1, u_2) has the form given in eqs (3 and 4).

where $Q(t)$ must be a non-zero quantity.

$$Q(t) = \frac{1}{V' \left(\frac{1}{V_T} v_2 - \frac{1}{V_T} x_1 \right) + \frac{\lambda'}{C_0} \left(\frac{1}{V_T} v_2 - \frac{1}{V_T} x_2 \right)}$$

where \hat{u}_1 is temperature change; \hat{u}_2 is moisture change.

The transfer functions of the FDP are as given in eqs (5 and 6). The G_{11} is derived from loop 1 and G_{22} is derived from loop 2.

$$G_{11} = \frac{0.00308}{0.0918 + s} \quad (5)$$

$$G_{22} = \frac{0.0938}{0.058 + s} \quad (6)$$

4 Design of different control schemes

The control objective is to get the desired performance and better quality in the drying of sliced pineapple. The different control schemes used for drying the sliced pineapple are IMC-PI, IMC-PI using GA and IMC-PI using PSO.

4.1 Conventional IMC-PI controller for single objective function

In the IMC scheme formulation, the controller, $q(s)$ is designed based on the part of the process transfer function that can be inverted. The IMC formulation generally results in only one tuning parameter λ , the IMC filter factor or closed loop time constant. The PI tuning parameters then become a function " λ ". The selection of tuning parameter (λ) is directly related to the robustness (sensitivity to model error) of the closed-loop system.

The feedback controller $g_c(s)$ contains the internal model $\tilde{g}_p(s)$ and internal model controller, $q(s)$. Currently, the IMC design procedure can be used to design a standard feedback controller. The standard feedback controller is a function of the internal model, $g_p(s)$ and internal model controller, $q(s)$ as given in eq. (7).

$$g_c(s) = \frac{q(s)}{1 - g_p(s) q(s)} \quad (7)$$

For a first-order process given in eq. (8), the PI controller settings are obtained using the eqs (9 and 10).

$$\tilde{g}_p(s) = \frac{K_p}{\tau_p s + 1} \quad (8)$$

$$K_c = \frac{\tau_p}{K_p \lambda} \quad (9)$$

$$K_I = \frac{K_c}{\tau_I} = \left[\frac{\tau_p}{K_p \lambda} \right] \left[\frac{1}{\tau_I} \right] \quad (10)$$

The desired value for λ is obtained by considering a trade-off between performance and robustness. The controller parameter values for the IMC-PI control scheme are determined by using the trial-and-error method and the values thus obtained are tabulated in Table 2.

Table 2: Controller parameter values for IMC-PI controller.

Controller	K_C	K_I
Temperature	0.8862	0.0987
Moisture	0.9452	0.1176

The comparison of performance measures for different values of λ is tabulated in Table 3.

Table 3: Comparison of performance measures for different values of λ .

λ	Temperature ISE	Moisture ISE
0.1107	28.73	44.83
0.1256	40.86	54.56
0.1345	45.98	58.97
0.1446	42.87	68.13
0.2341	39.05	50.31

In IMC-based PI, “ λ ” parameter selection using the trial-and-error method is time consuming process. Hence, λ is optimized using evolutionary algorithm, namely GA and PSO.

4.2 Evolutionary algorithm-based IMC-PI

PSO is a relatively recent heuristic search method whose mechanics are inspired by the swarming or collaborative behavior of biological populations. PSO is similar to the GA in the sense that these two evolutionary heuristics are population-based search methods. In other words, PSO and the GA move from a set of points (population) to another set of points in a single iteration with likely improvement using a combination of deterministic and probabilistic rules. The GA and its many versions have been popular mainly because of its intuitiveness, ease of implementation and the ability to effectively solve highly nonlinear, mixed integer optimization problems that are typical of complex engineering systems. The drawback of the GA is its expensive computational cost.

4.2.1 IMC-PI using GA for single-objective function

In solving a highly nonlinear problem, GA is preferred mainly because of its intuitiveness, ease of implementation and mixed integer optimization problems that are typical of complex engineering problems. To meet the desired specification, PI controller parameters are tuned by using an optimization technique [10, 11] namely, GA. The GA parameters used for tuning the GA-based IMC-PI scheme are given in Table 4.

Table 4: GA parameters used for tuning GA-based IMC-PI scheme.

Parameters	Values
Population size	10
Number of generations	20
Probability of crossover	0.99
Probability of mutation	0.01
Selection procedure	Ranking
Crossover type	Single point crossover
Objective function	ISE
Fitness function	Variance

The desired PI parameters around an operating point are generated randomly as the initial population. Each of these PI settings is applied to the system and the fitness of each chromosome is calculated. The chromosomes that are having the best fit value are taken to the next iteration whereas the chromosomes with the worst fit are discarded. The function of the crossover operator is to generate new “child” chromosomes from two “parent” chromosomes by combining the information extracted from the parents. The mutation operates individually on each chromosome by probabilistically perturbing each bit string. This process repeats until the desired performance index is met.

The objective function considered here is the ISE and the decision variables obtained are PI controller parameters, namely: K_C and K_I . The controller settings thus obtained for the IMC-PI controller scheme using GA are tabulated in Table 5.

Table 5: PI Controller parameter values for IMC-PI using GA ($\lambda=0.1107$).

Controller	K_C	K_I
Temperature	1.6133	0.0877
Moisture	1.6205	0.2671

The main drawback of GA is that it consumes more time for computation. This is alleviated using PSO-based optimization.

4.2.2 IMC-PI controller using PSO for single-objective function

In the design of an IMC-PI controller using PSO, the desired PI parameters, around an operating point, are generated through a bird flocking in two-dimensional space. The position of each agent is represented by the XY axis position and the velocity is expressed by V_x (velocity of X-axis) and V_y (velocity of Y-axis). Each of these PI settings is applied to the system; the velocity and position are calculated. From this, the best values are taken, and the agent position is realized by the position and velocity information [12]. The PSO parameters used for tuning the GA-based IMC-PI scheme are given in Table 6.

Table 6: PSO parameters used for tuning IMC-PI-based PSO scheme.

Parameters	Values
Sampling number, N	12
Local Attractors, C_1	2
Global Attractors, C_2	2
Objective function	ISE

The controller parameter values for the IMC-PI controller scheme using PSO are tabulated in Table 7.

Table 7: IMC-PI controller parameters obtained using PSO ($\lambda=0.1107$).

Controller	K_C	K_I
Temperature	1.6099	0.0297
Moisture	1.6097	0.0189

5 Closed loop analysis

The drying of sliced pineapple output responses, namely: the inside temperature and inside moisture, obtained by using three different control schemes for the linearized and decoupled model of the drying of sliced pineapple are shown below for servo and regulatory operation.

5.1 Servo operation

The simulation studies are performed to simulate the drying process of sliced pineapple. The output responses, namely: the temperature and moisture thus obtained by using three different control schemes are shown in Figure 3 and Figure 3 respectively.

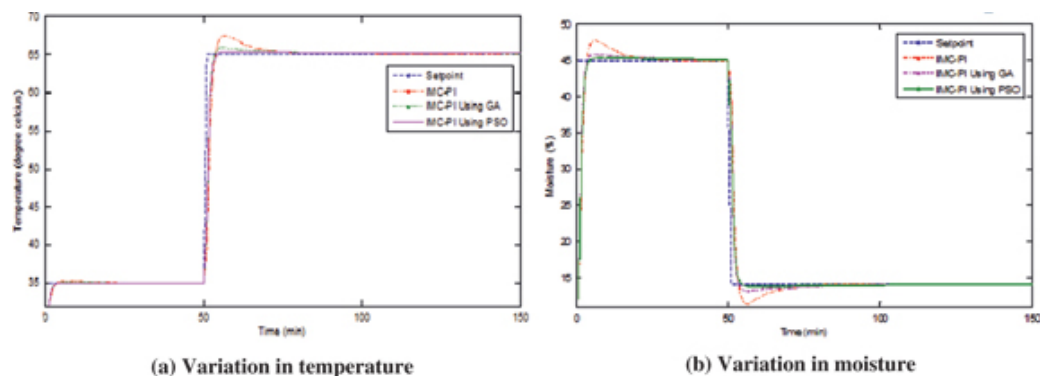


Figure 3: Comparison of closed loop performances of three types of IMC-PI controllers for servo operation.

From Figure 3 and Figure 3, it is observed that the performance of the IMC-PI controller tuned using PSO is better compared to other two control schemes. This is also reflected in the value of λ that is computed using the PSO-based optimization algorithm. The corresponding variations in the manipulated variables namely: the ventilation rate and heater are shown in Figure 4 and Figure 4, respectively. From these figures, it is observed that the variations in the manipulated variables are smooth.

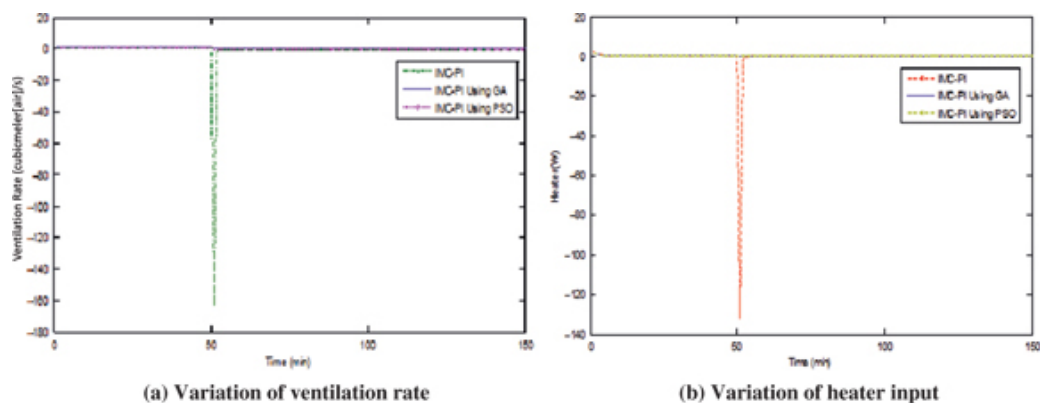


Figure 4: Corresponding variations in associated manipulated variable for servo operation.

5.2 Regulatory operation

The simulation studies are also extended to perform regulatory operations to reject the disturbances in temperature loop as well as in moisture loop.

5.2.1 For disturbance in temperature loop

Regulatory responses for the three types of IMC-PID controllers are obtained by providing a load change of 5 % at time $t = 100$ min on the temperature loop and the variations observed in temperature and moisture are shown in Figure 5 and Figure 5 respectively.

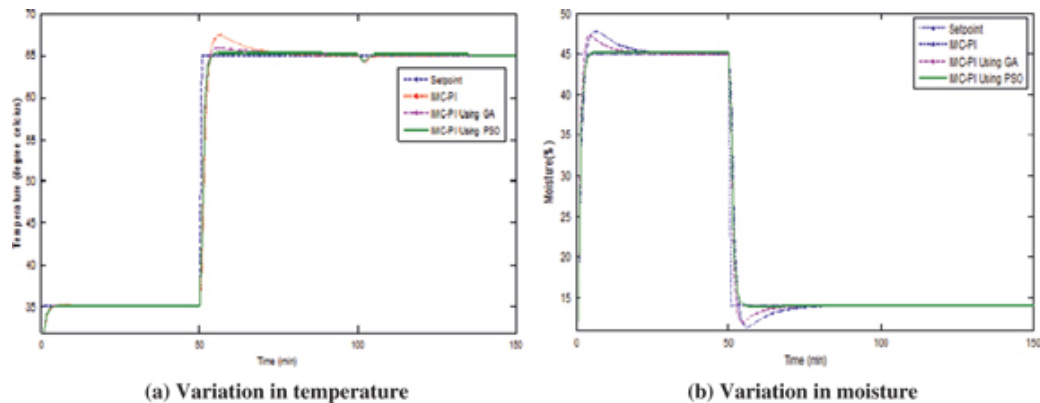


Figure 5: Comparison of closed loop performances of three types of IMC-PID controllers for regulatory operation (for disturbance in temperature loop).

It is observed that the performance of the IMC-PID controller tuned using PSO is better. The corresponding variations in manipulated variables, namely: the ventilation rate and heater output for a disturbance in the temperature loop at time $t = 100$ min are shown in Figure 6 and Figure 6 respectively. It is observed that the variations in the manipulated variables are smooth.

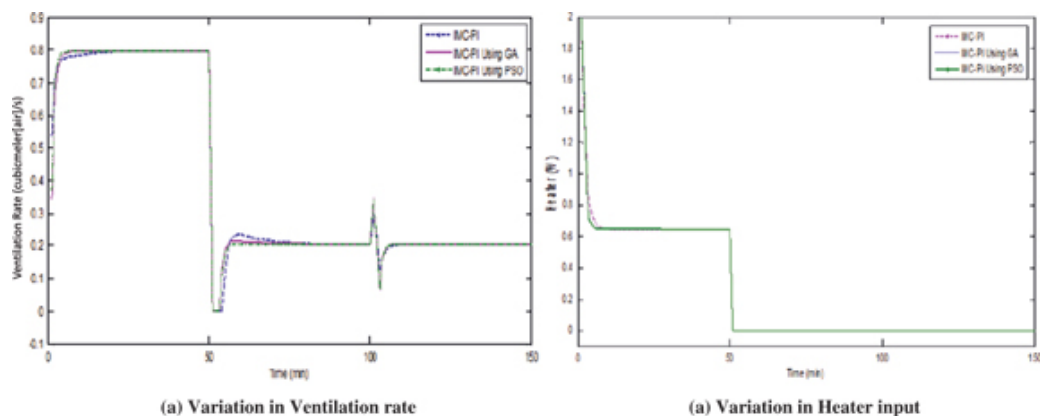


Figure 6: Corresponding variations in associated manipulated variable for regulatory operation (for disturbance in temperature loop).

5.2.2 For disturbance in moisture loop

In this case, the regulatory responses for the three types of IMC-PID controllers are obtained by providing a load change of 5 % at time $t = 100$ min on the moisture loop and the responses thus obtained are shown in Figure 7 and Figure 7 respectively. It is observed that the IMC-PID controller tuned using PSO has the minimum overshoot. The corresponding variations in the manipulated variables, namely: the ventilation rate and heater input, for a disturbance in the moisture loop at time $t = 100$ min are shown in Figure 8 and Figure 8 respectively. It is observed that the variations in the manipulated variables are smooth.

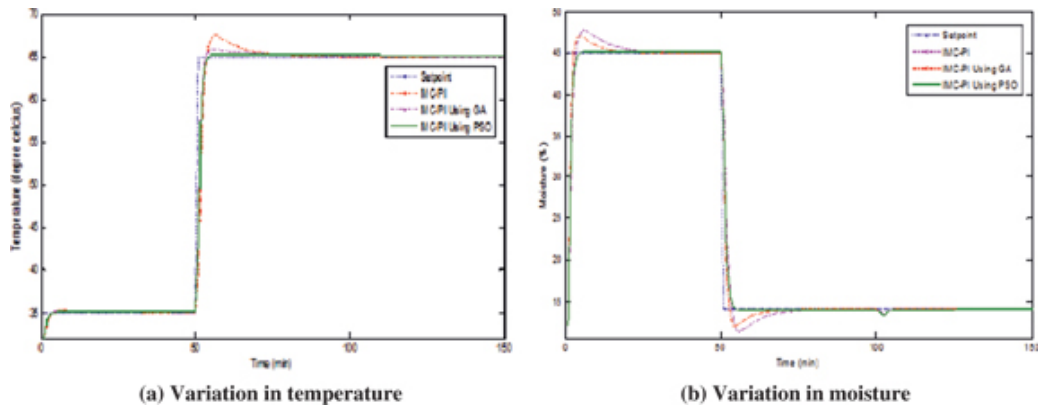


Figure 7: Comparison of closed loop performances of three types of IMC-PI controllers for regulatory operation (for disturbance in moisture loop).

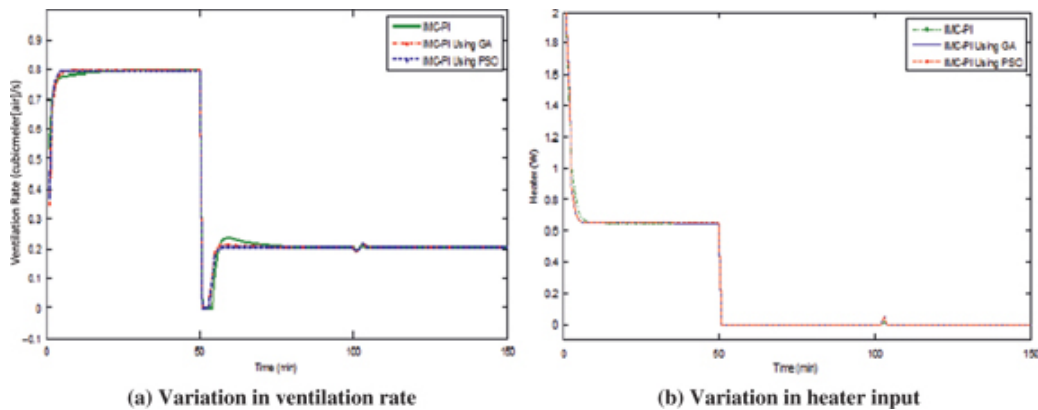


Figure 8: Corresponding variations in associated manipulated variable for regulatory operation (for disturbance in moisture loop).

From the three control schemes, it is inferred that IMC-based PI controller using PSO gives a better performance compared to other two control schemes. However, the control efforts in all the above control schemes are comparatively high. In order to achieve a minimum CE, a multi-objective approach is incorporated in the design of IMC-based PSO scheme.

5.2.3 Multi-objective control scheme for IMC-based PI for PSO

The multi-objective optimization methods have been around for at least past four decades. All the classical algorithms are preference-based approaches, where a relative preference vector is used to scalarize multiple objectives. Thus, suggested a way to convert a multi-objective optimization into a single-objective problem [13]. The most popular classical methods include: Weighted sum, ε -Constraint, Goal programming.

In the present work, the weighted sum approach is used for minimizing a weighted sum of multiple objectives. In this paper, minimum ISE and minimum CE are considered as two conflicting objectives. Thus, the weighted sum of the objective function is given by eq. (11),

$$\text{Error} = \alpha \text{ ISE} + (1 - \alpha) \text{ CE} \quad (11)$$

The performance measures for the IMC-PI controller, IMC-PI controller tuned using GA and IMC-PI controller tuned using PSO for the drying process are performed using the integral absolute error (IAE) and the ISE as given in eqs (12, 13), respectively.

$$\text{CE} = \int_0^{\infty} [u(t)]^2 dt \quad (12)$$

$$\text{ISE} = \int_0^{\infty} [e(t)]^2 dt \quad (13)$$

where ISE-Integral square error, α -weighing factor, CE - control effort.

The pareto-optimal front for IMC-based PI controller scheme using PSO is shown in Figure 9. The solutions are spread between the following extreme values: (1,425, 8.659) and (2,927, 11.19). Figure 9 shows that ISE (performance measure) and control effort (stability measure) are two conflicting objectives. Hence, the ISE is minimum and CE will be maximum and vice versa. From Figure 9, it is also inferred that for $\alpha = 0$, the objective function minimizes ISE, while for $\alpha = 1$, the objective function is maximum and for the intermediary values of α compromise both objectives.

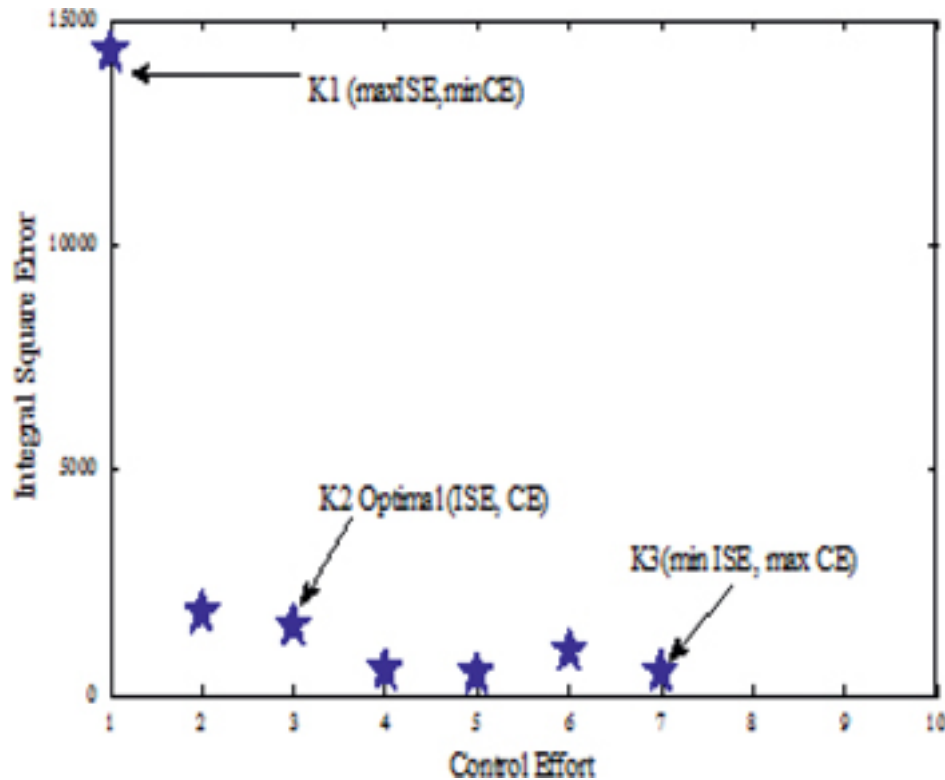


Figure 9: Pareto-optimal solutions obtained through PSO using weighted-sum method.

5.2.4 Quantitative comparison

The performance measures obtained for servo and regulatory operations (for disturbance in temperature loop and for disturbance in moisture loop) are tabulated in Tables (Table 8–Table 13) respectively.

Table 8: Comparison of performance measures obtained for servo operation (for variation in temperature).

Performance criterion	IMC-PI	IMC-PI Using GA	Temperature IMC-PI Using PSO
ISE	28.73	20.13	15.39
Overshoot (%)	2.29	0.756	0.54
Settling time (min)	35	25	15

Table 9: Comparison of performance measures obtained for servo operation (for variation in moisture).

Performance criterion	IMC-PI	IMC-PI using GA	Moisture IMC-PI using PSO
ISE	44.83	32.56	30.85
Overshoot (%)	3.66	2.726	2.24
Settling time (min)	34	28	17

Table 10: Comparison of performance measures obtained for regulatory operation (for variation in temperature with disturbance in temperature loop).

Performance criterion	IMC-PI	IMC-PI using GA	Temperature IMC-PI using PSO
ISE	29.76	21.14	20.29
Overshoot (%)	2.9	3.2	2.8
Settling time (min)	29	25	15

Table 11: Comparison of performance measures obtained for regulatory operation (for variation in moisture with disturbance in temperature loop).

Performance criterion	IMC-PI	IMC-PI using GA	Moisture IMC-PI using PSO
ISE	44.83	32.81	29.48
Overshoot (%)	3.66	2.726	2.34
Settling time (min)	31	28	20

Table 12: Comparison of performance measures obtained for regulatory operation (for variation in temperature with disturbance in moisture loop).

Performance criterion	IMC-PI	IMC-PI using GA	Temperature IMC-PI using PSO
ISE	28.71	20.46	19.3
Overshoot (%)	2.29	0.75	0.52
Settling time (min)	28	25.6	22.2

Table 13: Comparison of performance measures obtained for regulatory operation (for variation in moisture with disturbance in moisture loop).

Performance criterion	IMC-PI	IMC-PI using GA	Moisture IMC-PI using PSO
ISE	45.87	34.66	32.63
Overshoot (%)	3.67	2.73	2.24
Settling time (min)	25.5	24.3	20.5

From Table 8–Table 13, it is observed that the error is minimal for the IMC-PI controller tuned using PSO when compared to IMC-PI controller using GA and conventional PI controller. From these closed loop simulation studies, it is observed that the IMC-PI controller tuned using PSO gives better performance than the IMC-PI controller using GA and the IMC-PI controller for the drying of sliced pineapple. The comparison of performance measures and control effort for IMC-PI using PSO using the controller gain (K_1 , K_2 and K_3) is shown below in Table 14, for both single-objective and multi-objective operations.

Table 14: Performance comparison of three selected controller parameters obtained from pareto-optimal front.

IMC-PI using PSO	K_C	K_I	ISE	CE
Single-objective function	1.6099	0.0297	15.39	48.45
Multi-objective function	1.7143 1.7251 1.8453	0.0352 0.0321 0.0452	14,254 1,245 2,927	8.659 5.854 11.19

To achieve better performance K_1 (max (ISE) min (CE)) is selected, for optimal values of performance and control effort K_2 (optimal (ISE) optimal (CE)) is selected and to ensure stability K_3 (min (ISE) max (CE)) is selected.

6 Conclusion

In this work, IMC-based PI control scheme was developed for the drying of sliced pineapple to achieve desired temperature and moisture. For drying the sliced pineapple the temperature range considered is about 35 °C to 65 °C and the moisture range is about 45 %–14 %. The IMC-based PI control scheme is optimized using evolutionary algorithms namely: GA and PSO. The results implicate that a PSO-based IMC-PI controller provides better performance compared to conventional PI controller and the IMC-PI controller tuned using GA in drying the sliced pineapple with a minimum time period. As the disturbance occurring in one loop affects the performance of other loop, the decoupling is needed. This is obtained by using feedback-feedforward linearization technique. Then the multi-objective control problem is formulated to achieve minimum ISE and minimum CE, using weighted sum technique. This control scheme when used for drying of a sliced pineapple would result in quality of food during winter seasons. It is found from Table 14 that when ISE is minimum, the control effort will be maximum and vice versa (pareto-optimal front of multi-objective control scheme). Hence, the user can conveniently choose the best compromise solution from the pareto-optimal front to achieve the desired performance.

References

1. Hayakawa KI, Furuta T. Thermodynamically interactive heat and mass transfer coupled with shrinkage and chemical reaction . *Food Prop Comput-Aided Eng Food Proc Syst* 1998;1–6.
2. Yestitala B, Aktair MA. A simple moisture transfer model for drying of sliced food . *Appl Therm Eng* 2009;29(4):748–52.
3. Agarry SE, Ajani AO, Aremu MO. Thin layer drying kinetics of pineapple: effect of blanching temperature – time combination . *Niger J Basic Appl Sci* 2013;21(1):1–10.
4. Tan LW, Ibrahim MN, Kamil R, SaleenaTaip F. Empirical modeling for spray drying process of sticky and non-sticky products . *Procedia Food Sci* 2011;1:690–7.
5. Cordioli M, Rinaldi M, Copelli G, Casoli P, Barbanti D. Computational fluid dynamics (CFD) modeling and experimental validation of thermal processing of canned fruit salad in glass jar . *J Food Eng* 2015;150:62–9.
6. Padmavathi R, Anandharamakrishnan C. CFD Modeling of thermal processing of canned pineapple slices and titbits . *Food Bioproc Technol*, 2013:882–95. 64.
7. Lopez-Quiroga E, Vilas C, Alonso A. Time scale modeling and optimal control of freeze-drying . *J Food Eng* 2012;11(4):655–66.
8. Panda RC, RamachandraRao VS. Fluidized bed dryers: dynamic modelling and control . *Chem Eng Technol* 1991;14(5):307–10.
9. He F, Ma C. Modeling greenhouse air humidity by means of artificial neural network and principal component analysis . *Comput Electron Agric* 2010;71(1):S19–S23.
10. Cao YJ, Wu QH. Teaching genetic algorithm using matlab . *Int J Electr Eng Educ* 1999;36(2):139–53.
11. Liu WK, Juang JG. Application of genetic algorithm based on system performance index on PID controller . *Proc Ninth Conf Artif Intell Appl* 2004;2014:1–8.
12. Hasni A, Taibi DR. Optimization of greenhouse climate model parameters using particle swarm optimization and genetic algorithms . *Energy Procedia* 2011;6:371–80.
13. Deb K, Amrit P, Agarwal S, Meyarivan T. A fast and elitist multiobjective genetic algorithm: NSGA-II . *IEEE Trans Evol Comput* 2002;6(2):182–97.